

CZECH TECHNICAL UNIVERSITY IN PRAGUE,
FACULTY OF ELECTRICAL ENGINEERING

B2MPROJ6 - THESIS PROJECT

Inductive Wireless Power Transfer

Author

M. ŠIMÁK

DEPARTMENT OF

ELECTROMAGNETIC FIELD

Supervisor

Ing. J. KRAČEK, Ph.D.

DEPARTMENT OF

ELECTROMAGNETIC FIELD



February 2024

[THIS PAGE INTENTIONALLY LEFT BLANK.]

Contents

Introduction	2
1 Introduction to inductive wireless power transfer	3
1.1 Equivalent circuit analysis	3
2 Simulation of IWPT systems	4
2.1 Charts and atlases	4
2.2 Theoretical analysis	4
2.2.1 Length of the coils	4
2.2.2 DC resistance of the coils	5

Introduction

In recent years, the landscape of wireless power transfer (WPT) has undergone a significant transformation, fueled by the growing demand for convenient and efficient energy transfer methods in various industries. Among the plethora of wireless power transfer technologies, inductive wireless power transfer (IWPT) has emerged as a promising solution, particularly in the automotive sector. This project aims to delve into the fundamentals of inductive wireless power transfer, focusing on key aspects such as basic configuration, simulation of resistance and inductance, and a comparative analysis of simulation results against analytical formulas. The investigation also extends to the simulation of coils commonly employed in the automotive industry for mobile phone charging, utilizing exemplar coils provided by the esteemed collaboration with STMicroelectronics.

The automotive industry is undergoing a paradigm shift towards electric vehicles (EVs) and the integration of advanced technologies. As vehicles become more electrified, the demand for efficient and seamless methods of charging electronic devices within the vehicle, such as mobile phones, has intensified. Inductive wireless power transfer, characterized by the transmission of energy through magnetic fields, has garnered attention for its potential to provide a convenient and cable-free charging experience. This project addresses the burgeoning need for a deeper understanding of IWPT systems, their design parameters, and their application in the automotive domain.

Synopsis of the thesis. In **Chapter 1**, we aim to explore the basic configuration of inductive wireless power transfer systems. This chapter also introduces the tools for analysis of IWPT systems, such as equivalent circuit models.

Chapter 2 conducts simulations of resistance and inductance using ANSYS Maxwell software, with a particular focus on zero frequency (DC) scenarios. Further on, we compare simulation results with analytical formulas to validate the accuracy and reliability of the simulation model.

In conclusion, this thesis project represents a comprehensive investigation into the evolving field of inductive wireless power transfer, with a specific emphasis on its application within the automotive industry. The combination of theoretical exploration, simulation studies, and collaboration with industry leaders is poised to contribute valuable insights that will propel the advancement of wireless power transfer technologies in the automotive sector.

Methodology. The research methodology involves a step-by-step exploration of inductive wireless power transfer, starting with a theoretical foundation and progressing to detailed simulations using ANSYS Maxwell software. The comparison of simulation results with analytical formulas will provide a rigorous validation process. Additionally, the project will leverage the expertise and resources of STMicroelectronics for the simulation and analysis of coils relevant to automotive applications.

1. Introduction to inductive wireless power transfer

Chapter intro text...

1.1 Equivalent circuit analysis

Section intro text...

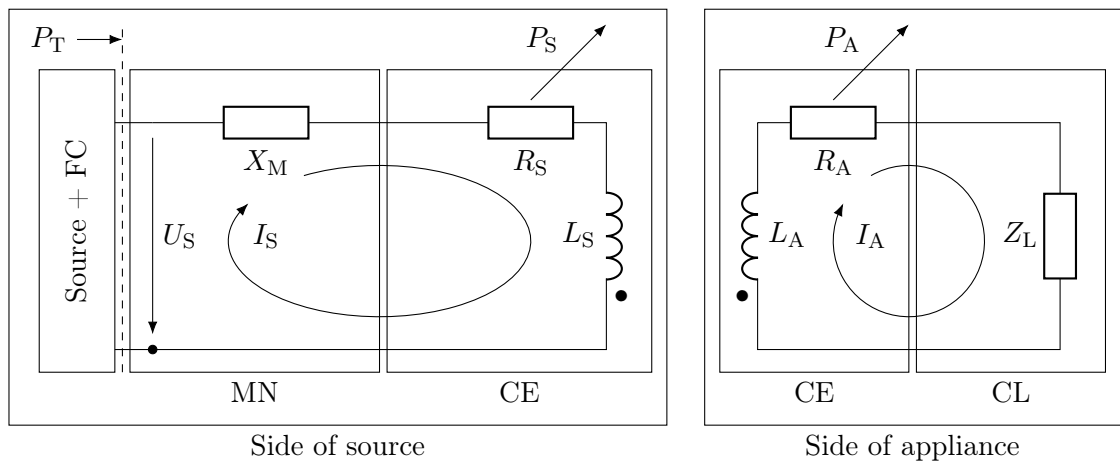


Figure 1.1: Circuit

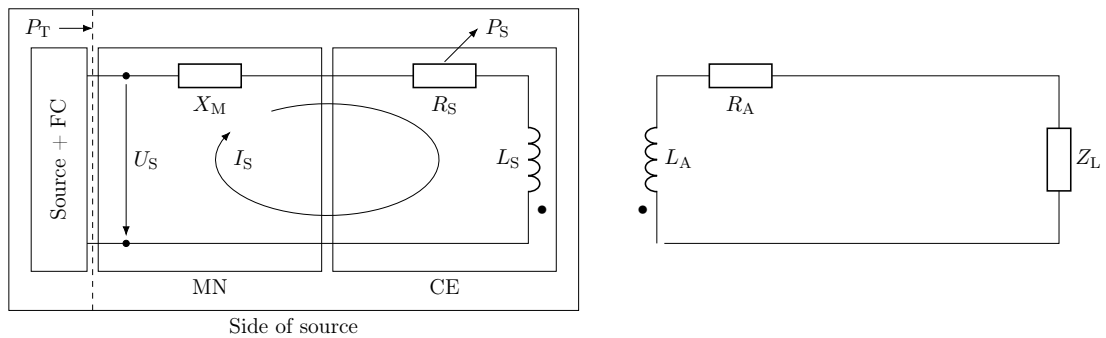


Figure 1.2: Circuit2

2. Simulation of IWPT systems

In the first chapter of this thesis, we introduce the concept of a smooth manifold. To readers experienced in topology, definition of the aforementioned might come across as trivial, but we consider it very important to specify how exactly we approach manifolds in general, since the underlying definitions might differ from text to text.

Apart from the smooth manifold itself, we will also introduce other key concepts of differential topology, such as charts, atlases, paracompactness, etc.

2.1 Charts and atlases

Before we begin, let us discuss the goal of this section. We would like to introduce a structure on a set that endows it with the property of “looking like” \mathbb{R}^n locally. In general, this will not be necessarily achievable globally on the whole set, but we will manage to arrive at a reasonable compromise using charts and atlases.

Definition 2.1.1. Let M be a set. A *chart* on M is a pair (U, \mathbf{x}) consisting of $U \subseteq M$ and an injective map $\mathbf{x} : U \rightarrow \mathbb{R}^n$ such that $\mathbf{x}[U] = \{\mathbf{x}(a) \mid a \in U\}$ is an open set in \mathbb{R}^n . The composite $x^i = \text{pr}_i \circ \mathbf{x} : M \rightarrow \mathbb{R}$ is often called the *i-th coordinate function*.

Note 2.1.2. Since \mathbf{x} , by definition, has \mathbb{R}^n as a codomain, we can always write its action upon a point $p \in M$ as $\mathbf{x} : p \mapsto \mathbf{x}(p) = (x^1(p), \dots, x^n(p))$. Whenever we wish to emphasize the individual coordinate functions, we write (x^1, \dots, x^n) or (x^i) instead of \mathbf{x} .

Remark 2.1.3. Note that we have defined charts on a plain set M . Therefore, we do not require U in (U, \mathbf{x}) to be open since we do not have the topological structure on M just yet.

2.2 Theoretical analysis

Some general talk...

2.2.1 Length of the coils

Underlying theorem. Let f be a function whose derivative is continuous on an interval $\alpha \leq \theta \leq \beta$. The arc length of the graph of $r = f(\theta)$ from $\theta = \alpha$ to $\theta = \beta$ is

$$\ell = \int_{\alpha}^{\beta} \sqrt{|f(\theta)|^2 + |f'(\theta)|^2} d\theta = \int_{\alpha}^{\beta} \sqrt{r^2 + \left(\frac{\partial r}{\partial \theta}\right)^2} d\theta. \quad (2.2.1)$$

Application. Since the *radius change* of the created spirals is 1.46 mm per turn, we can write the following formulas for the spiral curves of the transmitting and receiving coils:

$$r(\theta) = 10 + \frac{1.46}{2\pi}\theta, \quad 0 \leq \theta \leq N \cdot 2\pi, \quad (2.2.2)$$

where N is the number of turns of the respective coil. For such curves, we obtain

$$\ell_{\text{TxSpiral}} = \int_0^{10 \cdot 2\pi} \sqrt{\left(10 + \frac{1.46}{2\pi}\theta\right)^2 + \left(\frac{1.46}{2\pi}\right)^2} d\theta \text{ mm}, \quad (2.2.3)$$

$$\ell_{\text{RxSpiral}} = \int_0^{5 \cdot 2\pi} \sqrt{\left(10 + \frac{1.46}{2\pi}\theta\right)^2 + \left(\frac{1.46}{2\pi}\right)^2} d\theta \text{ mm}. \quad (2.2.4)$$

These formulas can then be evaluated, e.g. using *Wolfram Alpha*. The results are

$$\ell_{\text{TxSpiral}} = 1087.1 \text{ mm}, \quad \ell_{\text{RxSpiral}} = 428.9 \text{ mm}. \quad (2.2.5)$$

Result. For the total length of a coil, the feeding terminals must be taken into account:

$$\ell_{\text{TxTerminal1}} = 94.0 \text{ mm}, \quad \ell_{\text{RxTerminal1}} = 94.0 \text{ mm}, \quad (2.2.6)$$

$$\ell_{\text{TxTerminal2}} = 86.7 \text{ mm}, \quad \ell_{\text{RxTerminal2}} = 79.5 \text{ mm}. \quad (2.2.7)$$

Hence, the final length of the transmitting and receiving coils are

$$\ell_{\text{Tx}} = \ell_{\text{TxSpiral}} + \ell_{\text{TxTerminal1}} + \ell_{\text{TxTerminal2}} = 1.268 \text{ m}, \quad (2.2.8)$$

$$\ell_{\text{Rx}} = \ell_{\text{RxSpiral}} + \ell_{\text{RxTerminal1}} + \ell_{\text{RxTerminal2}} = 0.602 \text{ m}. \quad (2.2.9)$$

2.2.2 DC resistance of the coils

The DC resistance R of a wire of uniform cross-sectional area A , length ℓ and resistivity $\rho = \sigma^{-1}$, where σ is conductivity, can be calculated using the formula

$$R = \frac{\rho\ell}{A} = \frac{\ell}{\sigma A}. \quad (2.2.10)$$

We can apply this formula to our case of the aforementioned transmitting and receiving coils which consist of copper wire of cross-sectional area $A = 1 \text{ mm}^2$. The conductivity of annealed copper is $\sigma = 5.8001 \times 10^7 \text{ S m}^{-1}$. Altogether, we obtain the values of DC resistance

$$R_{\text{Tx}} = \frac{1.268}{5.8001 \cdot 10^7 \cdot 1 \cdot 10^{-6}} = 21.9 \text{ m}\Omega, \quad (2.2.11)$$

$$R_{\text{Rx}} = \frac{0.602}{5.8001 \cdot 10^7 \cdot 1 \cdot 10^{-6}} = 10.4 \text{ m}\Omega. \quad (2.2.12)$$

These results, compared with the simulation results of $R_{\text{Tx}} = 21.7 \text{ m}\Omega$ and $R_{\text{Tx}} = 10.5 \text{ m}\Omega$, verify the computational credibility of *ANSYS Maxwell*.